

## Research Article

<sup>1</sup>Department of Physics,  
McGill University, Montréal,  
QC, Canada

## Keywords

Oceanic sonar, climate change,  
underwater acoustics

## Email Correspondence

abigail.farkas@mail.mcgill.ca

<https://doi.org/10.26443/msurj.v19i1.203>

©The Authors. This article is  
published under a CC-BY license:  
<https://creativecommons.org/licenses/by/4.0/>

Abigail Farkas<sup>1</sup>

# The Effects of Climate Change on Oceanic Sonar Use in the Upper European Continental Shelf

## Abstract

As the global effects of climate change become more known year by year, it becomes ever-more pertinent to examine the effects this may bring for every aspect of modern life we rely on. One topic of focus is that of multi-frequency sonar communication and navigational systems, which rely on well-established relationships relating to wave speed, signal intensity, and attenuation. We compiled data on oceanic temperature, acidity, and salinity in the Upper European Shelf, which includes the North Sea and Mediterranean Sea, from 2006 to 2072 using the CMIP5 future climate model in the RCP8.5 scenario. We calculate that the speed of sound in the northern European oceanic area will decrease by almost 18 m/s by 2072, with an average yearly decrease in sound speed by 0.37 m/s. The attenuation of sound through water will change year by year, calculated based on a higher-order polynomial regression dependent on the frequency of sonar used. The maximum operating ranges of active low-frequency, mid-frequency, and high-frequency sonar systems would theoretically change by +0.06%, -0.19%, and +0.71%, respectively per year, if no other factors are affected. Due to increased sound propagation, the ambient noise level of the ocean would also increase and have some counter-effect to the increased detection range however that increase in noise level was not quantitatively analyzed in this study.

## Introduction

Multi-frequency sonar communication and navigational systems depend on being properly calibrated to the acoustical properties of the environment in which the sonar system is used. Rising global temperatures and other long-term changes in oceanic biomarkers may have a notable effect on the accuracy and effectiveness of these systems, and so analysis is required to determine the potential significance of these impacts and open a discussion into the topic.

Nautical navigational systems use either active or passive sonar in order to map their surroundings, locate marine life, or locate and communicate with other vessels at sea. Signal pulses from sonar systems can have a set frequency anywhere in the 1–200 kHz range, because different frequencies have different resolutions and can serve these various purposes better.

Active sonar consists of sending out these signal pulses, then listening for the returned signal that was reflected off of nearby vessels, sea life, or the ocean floor, and calculating the distance  $d$  based on the time  $t$  between the sent signal and the received reflection using the equation  $d = \frac{t \cdot c}{2}$  where  $c$  is the speed of sound in m/s.

Passive sonar is quite different, where the system only listens for any incoming acoustic signals emitted from any sources of interest with an array of sensors. Determining the distance from the vessel to the detected source employs a model of non-linear equations based on the differences in detection time at each sensor in the array. Passive sonar systems are less sensitive to changes in speed of sound, and so this analysis only pertains to active sonar.

A simplified 3rd order polynomial equation for the speed of sound under-water is given by Medwin (1975)<sup>1</sup>:

$$c \text{ (m/s)} = 1449.2 + 4.6T - 0.055T^2 + 0.00029T^3 + (1.34 - 0.010T)(S - 35) + 0.016D, \quad (1)$$

where  $T$  is temperature in °C,  $S$  is salinity in parts per thousand (ppt), and  $D$  is depth in meters (m). The variables must be within the parameters

$$0^\circ\text{C} \leq T \leq 35^\circ\text{C}, \quad 0 \text{ ppt} \leq S \leq 45 \text{ ppt}, \quad 0 \text{ m} \leq D \leq 1000 \text{ m}$$

for Medwin's equation to hold.

The effects from climate change on the effectiveness or accuracy of sonar systems can be theorized as follows: if the speed of sound through water varies due to rising temperatures, then the system may inaccurately calculate the distance of the object to the ship. If the attenuation of the signal through the ocean is higher than it is expected to be, then the range estimates generated by the sonar are reduced.

The change in accuracy of sonar is determined using Equation 1, and the change in effective range is determined using the sonar equation, which is the ratio of the sound intensity of the detected sonar signal that was emitted and reflected to the background noise present in the environment<sup>2</sup>:

$$SNR(\text{dB}) = SL - 2(TL_s + TL_a) + TS - NL. \quad (2)$$

Here,  $SNR$  is the Signal-to-Noise Ratio,  $SL$  is the source level,  $TL_c = 10 \log_{10}(\frac{d}{d_{ref}})$  is the transmission loss due to the cylindrical spread of sound where  $\frac{d}{d_{ref}}$  is the ratio of the initial reference distance\* to the distance over which the sound travels<sup>3</sup>,  $TL_a$  is the transmission loss due to attenuation,  $TS$  is the target strength, and  $NL$  is the noise level. More advanced navigational systems will use beamforming<sup>4</sup> to only listen for signals from a specific direction by using a spatial array of multiple receivers, effectively reducing the noise level and adding an additional term  $+AG$  for array gain<sup>5</sup>.

There is precedence in this area of research with regards to the effects of climate change on ecological life, such as bats, dolphins, and whales which

\*  $d_{ref}$  is set to a distance of 1 km in all subsequent calculations, as is standard for underwater acoustics applications<sup>2</sup>.

communicate in various ranges of frequency bands. One especially relevant and extensive study is that conducted by Luo et al. (2013) on the effects of global warming on echolocating bats<sup>3</sup>. They theorize that bats are altering the frequencies of their calls to compensate for the increase in atmospheric transmission loss used in Equation 2, given by

$$TL_a = \alpha(d - d_{ref}) \quad (3)$$

where  $d_{ref}$  (km) is the reference distance to the sound source from where the sound pressure would be measured,  $d$  (km) is the distance that sound travels, and  $\alpha$  (dB/km) is the atmospheric absorption coefficient, which is a function of frequency, air pressure, temperature, and relative humidity<sup>6</sup>.

Although the model formed by Luo et al. considers sonar frequencies travelling through air, the same concepts could also be directly applied to sonar travelling through water. Studies have also already shown that baleen whales, who typically operate in low frequencies (<100 Hz)<sup>7</sup>, are also decreasing the frequencies of their calls by a rate of more than 0.1 Hz per year<sup>8</sup>.

The main difference for applications of underwater acoustics is the definition of the absorption coefficient, which is now the seawater absorption coefficient defined as

$$\alpha = \alpha_{H_3BO_3} + \alpha_{MgSO_4} + \alpha_{H_2O} = \frac{A_1 P_1 f_1 f^2}{f_1^2 + f^2} + \frac{A_2 P_2 f_2 f^2}{f_2^2 + f^2} + A_3 P_3 f^2. \quad (4)$$

Here,  $\alpha_{H_3BO_3}$ ,  $\alpha_{MgSO_4}$ , and  $\alpha_{H_2O}$  are the absorption contributions from boric acid<sup>9</sup>, magnesium sulphate, and pure water<sup>10</sup>, respectively,  $A_1, A_2, A_3$  are constants,  $P_1, P_2, P_3$  are the pressure dependencies of each compound, and  $f_1, f_2$  are the relaxation frequencies of the two respective compounds. These are given by<sup>11</sup>

$$f_1 = 0.78 \sqrt{\frac{S}{35}} e^{\frac{T}{26}} \text{ kHz},$$

$$f_2 = 42 e^{\frac{T}{17}} \text{ kHz}.$$

With all constants and functions inputted, the coefficient becomes:

$$\alpha = 0.0827 \frac{\sqrt{\frac{S}{35}} e^{\frac{T}{26}} f^2}{0.0174 S e^{\frac{T}{14}} + f^2} e^{\frac{pH-8}{0.56}} + 0.52 \left(1 + \frac{T}{43}\right) \left(\frac{S}{35}\right) \frac{42 e^{\frac{T}{17}} f^2}{1764 e^{\frac{2T}{17}}} e^{-\frac{D}{6}} + 0.00049 f^2 e^{-\frac{T}{27} - \frac{D}{17}} \quad (5)$$

which now is dependent on salinity  $S$  (ppt), acidity  $pH$  (pH), depth  $D$  (km), sea temperature  $T$  (°C), and frequency  $f$  (kHz) in the given units.

Ainslie and McColm<sup>11</sup> further simplify this equation by using  $pH = 8$ ,  $S = 35$  ppt, and  $T = 10$  °C, however for the purposes of this study, the predicted change in these values are of importance to determine the increase of the  $\alpha$  coefficient, and thus the decrease of effective range.

## Methods

One location of interest had to be determined for this study, based on where changes in oceanic bio-markers such as temperature, salinity, and acidity change the most dramatically. This location should also be an area where sonar navigational systems are most critically used.

The main limiting factor in choice of location, however, was the ease of access and the extensiveness of available data for the region. We then decided that the region of interest would be the European shelf, which includes the North Sea and Mediterranean Sea. Vessel activity is typically most concentrated around bottlenecks and passages out to open water from ports with

high traffic and throughway channels, where it is most important for ships to get accurate sonar readings on their surroundings.

The data set we used was a POLCOMS-ERSEM product compiling marine biochemistry data in the European shelf from 2006 up to 2100, derived from CMIP5 climate projections<sup>12</sup>. We used the RCP8.5 “business-as-usual” future scenario model, in which current activities concerning greenhouse gas emissions continue to rise through the century. Data with parameters of acidity, salinity, and sea water potential temperature were pulled and analyzed, with a resolution of 1 month. The values pulled were at a depth of 5 meters from the ocean surface. Atlas figures were created to show trends of the typical variation of the biomarker value within one year, and the total change in average biomarker value in a specified span of time. These two trends will be compared and we will discuss whether the total change over time due to climate change has significant potential effects on sonar communications.

One-year variation is calculated using the known formula for standard deviation, and total changes in average values of temperature, salinity, and acidity are calculated using the following formula:

$$\Delta X = \frac{\sum \mu_N}{N} = \frac{\sum \frac{x_{N_i}}{12}}{N}, \quad (6)$$

where  $\frac{\sum x_i}{12}$  is the mean data value for a given year from twelve monthly data points and  $N$  is the number of years in the relevant time span of interest.

## Analysis

One-year variations in each of the biomarkers were analyzed quantitatively and then graphed, showing examples for one year in the past (2006) and present (2023). The total change in the average value for each of the biomarkers was analyzed using Equation 6 and then graphed for spans of time in the past (2006 – 2023) and in the future (2023 – 2072).

The overall trends in variation and average values were then plotted and we determined whether they had weak or strong correlation depending on the residuals of the data to a linear fit, as well as whether the trends accurately represent the entire region of interest.

Although the data spans 2006 to 2100, our analysis was limited to 2072 in order to find more conclusive and relevant results for the “near future” in the next 50 years. It was found that year-by-year, from 2023 to 2072, there will be an increase in oceanic temperature and a decrease in salinity and acidity in the upper European continental shelf.

### Temperature

The average sea water potential temperature is predicted to rise by approximately 1.2 °C in the next 50 years (Table 1). This change is of a smaller magnitude than that of the average variations of sea temperature in a given year, seen in Figure 5, and this yearly variation in temperature is also rising (Figure 2). In 2006, the sea temperature fluctuated by around 2.8 °C throughout the year. In 2072, temperatures are predicted to fluctuate by a little more than 3 °C during the year (Table 2). Fluctuations and long-term changes are seen across the entirety of the North Sea and Mediterranean Sea.

### Salinity

The changes in salinity are mostly restricted to the shorelines off of Norway and the Adriatic Sea surrounded by Italy and Croatia, as seen in Figure 6. It is important to note that from 2006 to the present, overall salinity had been

rising in the Adriatic Sea, yet also decreasing in the North Sea closer to where polar ice formations occur. However, there appears to be an overall decreasing trend in salinity with a 20-year periodicity cycle, which can be seen in Figure 3. In the next 50 years, there is a predicted drop in salinity by approximately 0.2 PSU (Practical Salinity Units)<sup>†</sup> across the wider region of the open ocean, as seen in Table 1. The predicted year with the lowest oceanic salinity will occur in 2045.

No concurrent explanation could be found for the periodic trend, however the overall decrease is corroborated by Junlin et al. (2023) looking at salinity trends in the Pacific Ocean from 2005 to 2019<sup>13</sup>, and by Bagnell et al. (2023) studying global oceanic trends from 2001 to 2019<sup>14</sup>. Bagnell presents the correlation of steady, decreasing salinity with dilution due to the melting of icecaps, which introduce more freshwater into the oceans. Thus, we can speculate that the overall predicted change could be due to the disappearance of all ice formations. This aligns with some of the latest research conducted on when the world will first see ice-free summers, predicted to be in the 2030s – 2050s<sup>15</sup>.

### Acidity

Overall acidity in the ocean is expected to decrease – becoming more acidic – in the next 50 years. This is a widely confirmed trend known as *ocean acidification* and is attributed to rising dissolved CO<sub>2</sub> levels<sup>16</sup>. The changes in acidity modelled from the dataset are concentrated to the north shoreline of the Western Mediterranean Basin, right in the French Gulf of Lion as seen in Figure 7. There is a clear trend of decreasing acidity year by year (Table 1) and in comparison the yearly acidity fluctuates at varying magnitudes year by year (Figure 4). Thus, the yearly variation has a statistically weak trend but the change in average acidity over time is still statistically significant.

## Results

### Accuracy

Using the yearly changes of each biochemical marker which showed strong trends, the changes in speed of sound (Equation 1) and transmission loss (Equation 5) through the ocean were calculated over the 50-year span, which were then used to determine the percentage decreases of accuracy and efficacy each year.

We calculated that the speed of sound in the relevant oceanic area will decrease by almost 18 m/s from 2023 to 2072, with an average yearly decrease in sound speed by about 0.37 m/s. This, in turn, implies that if an active sonar system is not re-calibrated it would decrease in accuracy by approximately 0.025% every year, and will read that objects are farther away due to the longer return time of the signal pulse — for example, if a new sonar instrument installed in 2006 originally measured an obstacle to be exactly 40 meters away, it would now measure that same obstacle to be at a distance of about 40.17 meters in 2023.

However, it is typical for sonar systems which critically rely on accurate sound speed to operate an on-board independent sound speed sensor in order to measure the exact local oceanic sound speed. We can assume that the possibility of a vessel's sonar navigational system to spend multiple years without recalibration is extremely unlikely.

Additionally, in comparison to the predicted long-term condition changes, currently there is an average variation of  $\pm 2.763$  °C and  $\pm 0.193$  ppt in the ocean throughout a given year. This implies that there is currently a higher yearly variability of 0.52% in an instrument's accuracy than what is pre-

<sup>†</sup>The sourced data<sup>12</sup> measures salinity in PSU, which is interchangeable with ppt. Calculations will reference salinity in ppt with no note for the change from PSU.

dicted by change over time.

### Efficacy

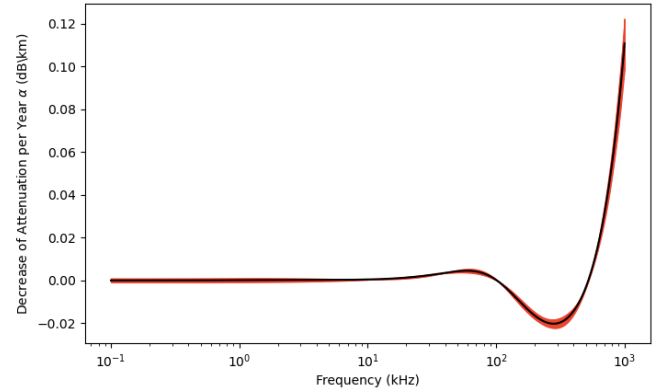


**Figure 1.** 11-order polynomial regression of the decrease in attenuation per year based on frequency. The red area denotes the error of the curve fit in addition to the 10% uncertainty of the absorption coefficient equation<sup>11</sup>.

The seawater absorption coefficient  $\alpha$  of transmission loss  $TL_a$  was approximated to be decreasing by an 11th order polynomial fit to Equation 5:

$$\begin{aligned} \alpha(f) = & (-7.55 \cdot 10^{-31})f^{11} + (4.34 \cdot 10^{-27})f^{10} - (1.09 \cdot 10^{-23})f^9 \\ & + (1.55 \cdot 10^{-20})f^8 - (1.38 \cdot 10^{-17})f^7 + (7.92 \cdot 10^{-15})f^6 \\ & - (2.91 \cdot 10^{-12})f^5 + (6.52 \cdot 10^{-10})f^4 - (7.51 \cdot 10^{-8})f^3 \\ & + (2.20 \cdot 10^{-6})f^2 + (1.14 \cdot 10^{-4})f - 8.65 \cdot 10^{-4} \end{aligned} \quad (7)$$

pertaining to the decrease in attenuation each year for frequencies between 100 Hz and 1 MHz, where  $\alpha(f)$  is in dB/km and  $f$  is in kHz.

It can be seen for mid-range frequencies between 100 kHz and 500 kHz that attenuation will increase (Figure 1). This is the range in which the largest effect on attenuation is determined from contributions of magnesium sulphate<sup>10</sup>. Below that frequency range, the decrease of attenuation remains relatively stable around  $10^{-3}$  dB/km where the largest contributor is boric acid<sup>9</sup>. In the highest frequency range, there is an exponential increase in attenuation loss due to viscous absorption<sup>11</sup>.

The percentage change in attenuation represents the inverse percentage change in maximum detection distance, seen by how a decrease in seawater transmission loss leads to an increase of *SNR* at a minimum detectable level for a longer distance. And so, determining the average effects on each of these three ranges separately, the maximum operating ranges would theoretically be increasing by 0.06% for low-frequency sonar (100 Hz – 100 kHz), decreasing by 0.19% for mid-frequency sonar (100 kHz – 500 kHz), and increasing by 0.71% for high-frequency sonar (>500 kHz) every year, if the ambient noise level in the ocean did not change as well. However, the increase of all underwater sound propagation would be another factor to consider for determining the overall impact on the long-term changes to the maximum range of sonar at different frequencies.

## Discussion

The results from this analysis can be compared to those found by Possenti et al. (2023)<sup>17</sup> in their examination of the wider topic of the effects of climate change on underwater sound propagation. They concluded that while there is a future projected (2094 to 2098) global increase in underwater sound

speed, the North Atlantic Ocean and Norwegian Sea would uniquely see a decrease in sound speed by as much as 40 m/s from 2022. This is almost double the predicted decrease in sound speed in this analysis, which was determined to be closer to a 27 m/s drop in speed by 2094.

This discrepancy could possibly be attributed to the different methods of future projection modelling, where Possenti et al. took just four years of past data and projected it to four years of future data using the SSP5-8.5 future scenario. They also use a 6th order polynomial approximation of the speed of sound in water model given by<sup>18</sup>

$$c_{s,bous} = \sqrt{\frac{-\rho_0 g}{\frac{\partial r_0}{\partial z} - \frac{1}{z_u} \frac{\partial r}{\partial \zeta}}} \quad (8)$$

where  $\rho_0$  is a constant reference density,  $z_u$  is a reference depth,  $r_0(z)$  is a vertical reference profile,  $r(S_A, \Theta, z)$  is a residual function, and  $\zeta = -\frac{z}{z_u}$ . In regards to the effective operating range of sonar detection and the decrease in attenuation, Possenti et al. find that there will be an increase in noise level  $NL$  by 7 dB by the end of the century. They come to the conclusion that propagation of ship noise in water will increase in the future, however they only examine single frequency at 125 Hz to find a total change in absorption coefficient of 0.0016 dB/km by 2094. Using our  $\alpha(f)$  function, we calculate a decrease of  $3 \cdot 10^{-6} \pm 0.0008$  dB/km per year. The uncertainty is beyond  $2\sigma$ , which implies that our result does not have sufficient confidence.

Regardless, determining a frequency-dependent function for the decrease in seawater absorption coefficient per year allows for application in all ranges of sonar, from low-frequency naval operations to fishfinding and seabed mapping.

It should also be noted that this analysis was limited to a depth of 5 m below sea level, at which there is more variability in biomarkers over shorter time frames.

## Conclusions

We conclude based on the isolated analysis conducted on changing oceanic temperature, salinity, and acidity in the upper European continental shelf, that the decrease in oceanic sound speed and subsequent decrease in accuracy in sonar navigation may be negligible when compared to the normal yearly fluctuations, and while it was quantitatively found that the change in transmission loss is frequency-dependent, the overall change in range of sonar detection is unknown due to the potential counter-effect of increases in ambient oceanic noise level.

Future research on this topic could include further analysis with the higher-order speed of sound model (Equation 8), as well as consider different depths in order to create a more comprehensive four-dimensional model of future conditions. Finally, analysis could be expanded to different areas of ocean to compare trends and put results into the global context.

## Acknowledgements

This research was made possible from the teachings and encouragement of Prof. Yi Huang, as well as the aid from Qiurun Yu as a Teaching Assistant.

## References

1. Medwin, H. Speed of sound in water: A simple equation for realistic parameters. *J. Acoust. Soc. Am.* **58**, 1318–1319 (1975). <https://doi.org/10.1121/1.380790>
2. Urick, R. J. *Principles of Underwater Sound* (Peninsula Publishing, 1984).
3. Luo, J., Koselj, K., Zsebok, S., Siemers, B. M. & Goerlitz, H. R. Global warming alters sound transmission: differential impact on the prey detection ability of echolocating bats. *J. R. Soc. Interface* **11**, 20130961 (2013). <https://doi.org/10.1098/rsif.2013.0961>
4. Chiang, A. M. & Broadstone, S. R. Sonar beamforming system (2005). US Patent 6,842,401.
5. Yan, L., Meng, Z., Chen, Y., Zhou, Z. & Chen, M. Vertical correlation and array gain analysis for vertical line array in deep water. *Appl. Sci.* **10**, 4709 (2020). <https://doi.org/10.3390/app10144709>
6. Attenborough, K. in *Springer Handbook of Acoustics* (ed Rossing, T. D.) 117–155 (Springer, 1979).
7. Adam, O. et al. New acoustic model for humpback whale sound production. *Appl. Acoust.* **74**, 1182–1190 (2013). <https://doi.org/10.1016/j.apacoust.2013.04.007>
8. Leroy, E. C., Royer, J. Y., Bonnel, J. & Samaran, F. Long-term and seasonal changes of large whale call frequency in the southern Indian Ocean. *J. Geophys. Res.* **123**, 8568–8580 (2018). <https://doi.org/10.1029/2018JC014352>
9. Francois, R. E. & Garrison, G. R. Sound absorption based on ocean measurements. Part II: Boric acid contribution and equation for total absorption. *J. Acoust. Soc. Am.* **72**, 1879–1890 (1982). <https://doi.org/10.1121/1.388673>
10. Francois, R. E. & Garrison, G. R. Sound absorption based on ocean measurements: Part I: Pure water and magnesium sulfate contributions. *J. Acoust. Soc. Am.* **72**, 896–907 (1982). <https://doi.org/10.1121/1.388170>
11. Ainslie, M. A. & McColm, J. G. A simplified formula for viscous and chemical absorption in sea water. *J. Acoust. Soc. Am.* **103**, 1671–1672 (1998). <https://doi.org/10.1121/1.421258>
12. Kay, S., Clark, J., Hall, A., Marsh, J. & Fernandes, J. Marine biogeochemistry data for the Northwest European Shelf and Mediterranean Sea from 2006 up to 2100 derived from climate projections. *Copernicus Climate Change Service (C3S) Climate Data Store (CDS)* <https://doi.org/10.24381/cds.dcc9295c> (2020).
13. Junlin, R., Chao, N., Wang, Z., Wu, T., Li, C., et al. Quantifying the contribution of temperature, salinity, and climate change to sea level rise in the Pacific Ocean: 2005–2019. *Front. Mar. Sci.* **10**, 1200883 (2023). <https://doi.org/10.3389/fmars.2023.1200883>
14. Bagnell, A. & DeVries, T. Global mean sea level rise inferred From ocean salinity and temperature changes. *Geophys. Res. Lett.* **50**, e2022GL101004 (2023). <https://doi.org/10.1029/2022GL101004>
15. Kim, Y. H., Min, S. K., Gillett, N. P., Notz, D. & Malinina, E. Observationally-constrained projections of an ice-free Arctic even under a low emission scenario. *Nat. Commun.* **14**, 3139 (2023). <https://doi.org/10.1038/s41467-023-38511-8>
16. Doney, S. C., Fabry, V. J., Feely, R. A. & Kleypas, J. A. Ocean acidification: the other CO2 problem. *Ann. Rev. Mar. Sci.* **1**, 169–192 (2009). <https://doi.org/10.1146/annurev.marine.010908.163834>
17. Possenti, L. et al. Predicting the contribution of climate change on North Atlantic underwater sound propagation. *PeerJ* **11**, e16208 (2023). <https://doi.org/10.7717/peerj.16208>
18. Roquet, F., Madec, G., McDougall, T. J. & Barker, P. M. Accurate polynomial expressions for the density and specific volume of seawater using the TEOS-10 standard. *Ocean Model.* **90**, 29–43 (2015). <https://doi.org/10.1016/j.ocemod.2015.04.002>

**Table 1.** Average values for seawater temperature, salinity, and acidity in 2006, 2023, and predicted 2072 values, as well as the average change over 65 years (Figure 4).

Year	One-Year Average		
	$\bar{T}$	$\bar{S}$	$\bar{pH}$
2006	15.91 °C	36.10 PSU	8.175
2023	16.19 °C	36.17 PSU	8.165
2072	17.48 °C	35.89 PSU	8.134
Yearly Change in Average (2006–2072)	+0.021 °C	-0.0065 PSU	-0.00072

**Table 2.** Yearly variation of seawater temperature, salinity, and acidity in 2006, 2023, and predicted 2072 values, as well as the change in variation over 65 years (Figure 4).

Year	One-Year Variation		
	$\sigma_T$	$\sigma_S$	$\sigma_{pH}$
2006	±2.757 °C	±0.196 PSU	±4.670
2023	±2.763 °C	±0.193 PSU	±2.618
2072	±3.072 °C	±0.207 PSU	±3.086
Yearly Change in Variation (2006–2072)	+0.003 °C	+0.0002 PSU	-0.00006

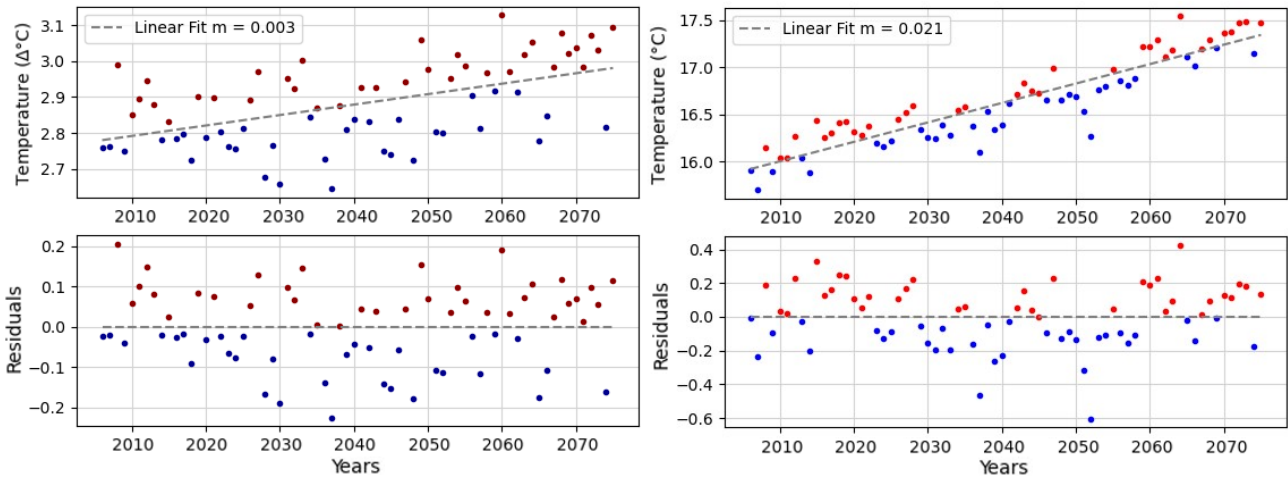


**Figure 2.** Linear regressions and residuals of yearly sea water potential temperature ( $^{\circ}\text{C}$ ) and fluctuation of sea water potential temperature ( $\Delta^{\circ}\text{C}$ ) in the European Shelf at a depth of 5 meters, from 2006 to 2072.

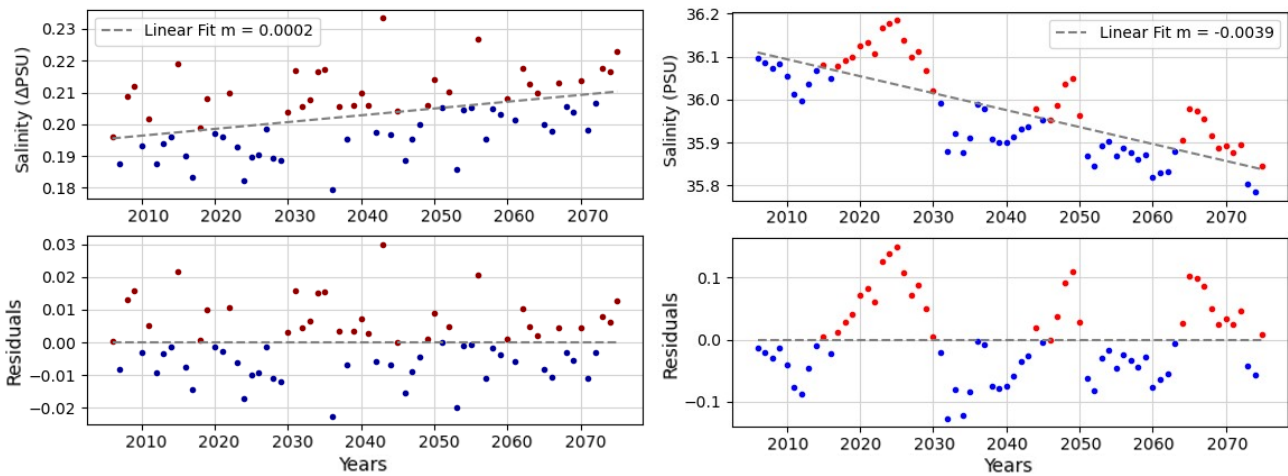


**Figure 3.** Linear regressions and residuals of yearly sea water salinity (PSU) and fluctuation of sea water salinity ( $\Delta\text{PSU}$ ) in the European Shelf at a depth of 5 meters, from 2006 to 2072.

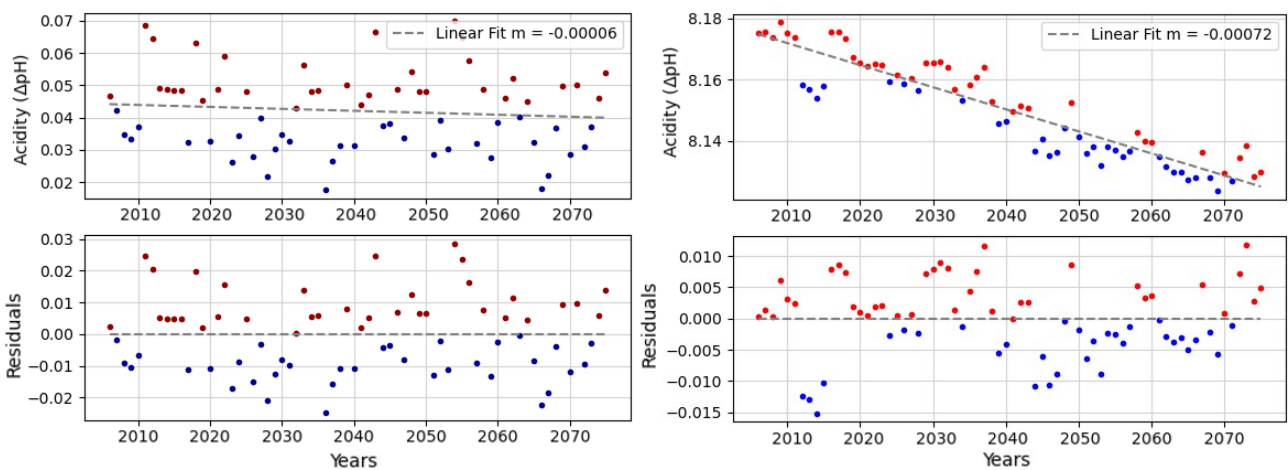


**Figure 4.** Linear regressions and residuals of yearly sea water acidity (pH) and fluctuation of sea water acidity ( $\Delta\text{pH}$ ) in the European Shelf at a depth of 5 meters, from 2006 to 2072.

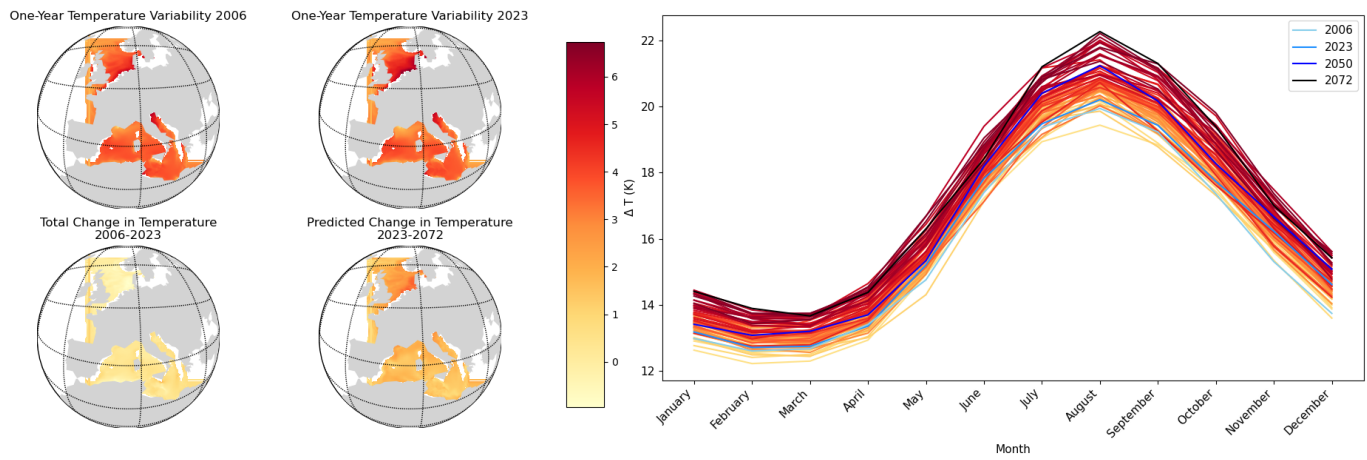


**Figure 5.** Geographical and yearly line trends of sea water potential temperature ( $^{\circ}\text{C}$ ) in the European Shelf at a depth of 5 meters, from 2006 to 2072.

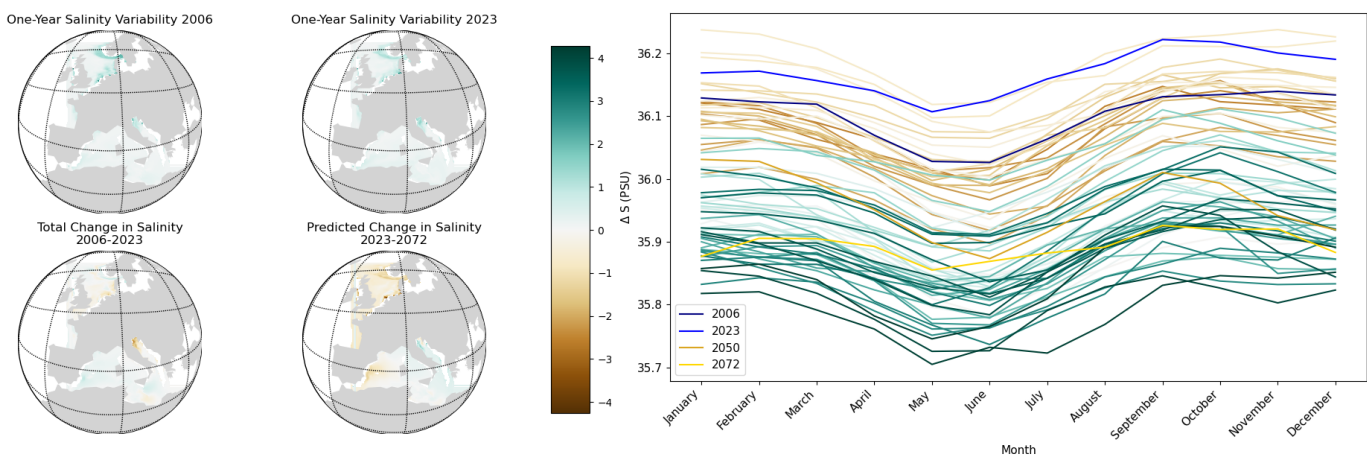


**Figure 6.** Geographical and yearly line trends of sea water salinity (PSU) in the European Shelf at a depth of 5 meters, from 2006 to 2072.

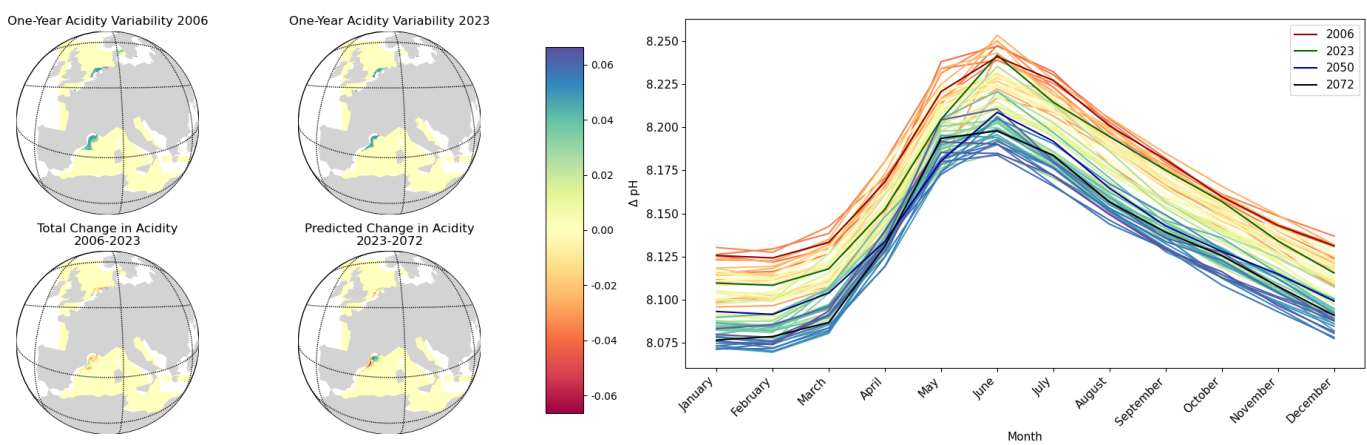


**Figure 7.** Geographical and yearly line trends of sea water acidity (pH) in the European Shelf at a depth of 5 meters, from 2006 to 2072.